

Journal of Rehabilitation in Civil Engineering

Journal homepage: https://civiljournal.semnan.ac.ir/

Fire Resistance and Collapse Mechanisms of 2D Steel Moment Frames: A Numerical Study

Arezoo Asaad Samani 10; Seyed Rohollah Hoseini Vaez 2,* 10

- 1. Ph.D. Candidate, Department of Civil Engineering, Faculty of Engineering, University of Qom, Qom, Iran
- 2. Professor, Department of Civil Engineering, Faculty of Engineering, University of Qom, Qom, Iran
- * Corresponding author: hoseinivaez@gom.ac.ir

ARTICLE INFO

Article history:

Received: 09 February 2025 Revised: 02 March 2025 Accepted: 16 March 2025

Keywords: Fire scenarios; Fire resistance; Collapse mechanisms; Steel moment frames.

ABSTRACT

This study investigates the behavior of steel moment-resisting frames under fire conditions, focusing on the structural response of three- and nine-story frames exposed to high temperatures. The analysis evaluates the effects of elevated temperatures deflections, internal forces, and inter-story drifts. Various fire scenarios are considered, with a fire duration of 120 minutes and a maximum temperature of 1050°C. The results reveal significant inter-story drifts, deflections in mid span of beams and substantial changes in internal forces of beams and columns. The columns are highly susceptible to buckling due to thermal expansion and reduced material properties. The results highlight the importance of focusing on columns and lower-to-mid-level stories in fire safety evaluations, as these components are more prone to failure and can significantly influence the overall structural stability. The strengths of this study lie in its thorough analysis of multiple fire scenarios and its precise identification of critical failure points, offering a robust foundation for advancing fire-resistant design methodologies. These findings have significant practical implications, as they provide engineers with valuable insights for enhancing the safety and performance of steel moment-resisting frames under fire conditions.

E-ISSN: 2345-4423

© 2025 The Authors. Journal of Rehabilitation in Civil Engineering published by Semnan University Press. This is an open access article under the CC-BY 4.0 license. (https://creativecommons.org/licenses/by/4.0/)

How to cite this article:

Asaad Samani, A. and Hoseini Vaez, S.R. (2026). Fire Resistance and Collapse Mechanisms of 2D Steel Moment Frames: A Numerical Study. Journal of Rehabilitation in Civil Engineering, 14(1), 2269. https://doi.org/10.22075/jrce.2025.36843.2269

1. Introduction

Fire is one of the serious hazards that can have devastating consequences, including loss of human life, destruction of property, and extensive economic losses. A thorough and comprehensive examination of fire and the assessment of factors influencing its spread are of paramount importance, as these investigations can aid in the implementation of preventive measures and fortification of structures. Furthermore, understanding fire behavior and its influence on structures enables engineers and building designers to apply safety regulations more accurately and to develop more effective emergency problems for evacuation and firefighting. Consequently, the significance of studying fires extends beyond protecting lives and property; It also raises safety standards and improves community resilience to disasters. The effects of fire on steel structures pose one of the fundamental challenges in the design and safety of buildings due to the thermal and mechanical properties of steel. As a robust and commonly used material in construction, steel loses its mechanical properties when subjected to extreme heat from fires, which can lead to a reduction in structural resistance and ultimately result in collapse. One of the critical effects of changes in the mechanical properties of steel on structural integrity includes alterations in the deflection and deformation of beams. Generally, during a fire, steel beams undergo thermal expansion, leading to an increase in their length and deflection. If the deflection exceeds permissible limits, the failure of the beam and potentially its collapse under additional loads will be occured. Controlling excessive deflection is a fundamental aspect of designing structures to withstand fire conditions in order to prevent collapse and irreparable damage. Building standards in many countries provide specific regulations for controlling deflection, strengthening, and designing steel structures against fire. Numerous studies have been conducted on the effects of fire on buildings [1–17].

In 2013, Jiang and usmani developed the OpenSees software for analyzing steel structures under fire conditions. They incorporated new functions into the material and section definition modules to calculate thermal loads, enabling nonlinear analyses that consider changes in mechanical properties due to increasing temperatures. Ultimately, they compared their results with the outputs of the Abaqus finite element software. Using their analytical methods, users can define temperature-dependent material properties and simulate non-uniform temperature distributions along the section and length of the member [18]. In 2014, Jiang et al. examined the resistance of steel structures to progressive collapse caused by fire by proposing a simplified design method. They investigated progressive collapse mechanisms in steel structures under fire conditions using the OpenSees software. After validating their analytical results with available laboratory data, they studied factors influencing progressive collapse, including beam strength, loading conditions, lateral bracing, and fire scenarios. They found that different fire scenarios significantly affect the type of collapse in steel structures [19]. In 2015, Elhami khorasani et al. added a new thermal module in OpenSees for analyzing steel structures subjected to fire, including postearthquake fire events. This new thermal module allows for structural analyses considering the effects of combined events such as fire following an earthquake. They also developed reliability analysis tools within the thermal module. Ultimately, these modifications facilitate non-uniform temperature distribution along an element and simplify the definition of temperature-dependent material properties for users [20]. In another study in 2015, Jiang et al. investigated the impact of different bracing frames on the resistance of steel structures to progressive collapse due to fire. Considering several fire scenarios, they modeled two types of bracing systems in the OpenSees software for fire conditions. They identified four collapse mechanisms for steel frames under fire and ultimately proposed a combination of vertical and diagonal braces as a safer design strategy for practical applications [21].

In 2020, Ren investigated the performance of steel frames under various fire spread scenarios. The study initially examined the impact of thermal protection on beams and its effect on the fire resistance of heated columns. Subsequently, the performance of three-dimensional steel frames was evaluated under the influence of seven different fire scenarios. The study assessed the effects of the timing of fire spread, its

direction, and the position of the fire source on the fire resistance of the steel frame. According to the results, due to the short duration of heating in the fire scenarios considered, thermal protection for beams had minimal impact on the performance of the heated columns [22]. In 2021, Jiang et al. conducted a study that explored the thermal analysis framework of OpenSees for assessing structural responses to fire, introducing a smart interface for modeling natural fire using Python-OpenSees. This framework was validated through uniform and localized fire tests, and it enabled realistic modeling of localized and moving fires. The results indicated that to more accurately describe the effects of natural fire, additional variables should be considered in the modeling, and the proposed framework possesses potential for future enhancements [23]. In 2022, Qiu et al. introduced a computational method for modeling composite slabs under fire conditions. The primary objective was to simplify and enhance the accuracy of modeling these slabs due to their complex performance. In their proposed method, a single reference surface was utilized in the shell element modeling to facilitate the adjustment of composite slabs, with ribbed sections and conical steel profiles defined integrally in the section. Additionally, to achieve a more realistic temperature distribution, the temperature was internally and automatically distributed among the various layers of the composite slab. The results demonstrate that this approach performs well in modeling composite slab systems under thermal and mechanical loading. This method not only provides high accuracy but also significantly simplifies the modeling process for multi-story buildings during fire conditions [24]. In 2022, Mortazavi et al. conducted a study comparing the thermal performance of eccentric braced frames (EBFs) and moment-resisting frames. They developed analyses for heat transfer and introduced new features in the element and material definitions within OpenSees for thermal analysis. They evaluated and improved the performance of the frames against thermal effects, ultimately simulating and analyzing several fire scenarios for both frame types. The results indicated that as the time to collapse due to fire increased, EBFs enhanced the fire performance of the system [25].

In 2023, Chen et al. focused on developing models for wooden structures affected by real fire in the OpenSees software. Utilizing the provisions related to timber structures in Eurocode 5, they investigated the behavior of wooden structures under fire conditions. They carried out developments on the OpenSees open-source platform, enabling the modeling of heat transfer in wooden sections and thermomechanical analyses for various wooden elements, such as beams and shells. Additionally, thermal measures for wooden slabs and beams exposed to fire on three sides were developed for these models [26]. In 2024, Mortazavi et al. examined the performance of eccentric braced frames (EBF) in low-rise buildings under various fire scenarios. In this study, they assessed the performance of low-rise structures with this type of brace. They designed a three-story building with an eccentric braced frame system and analyzed its behavior under six different fire scenarios. For the structural analysis under fire loads, the temperature distribution in fire-exposed members was initially evaluated using a finite element heat transfer analysis method. Subsequently, utilizing a nonlinear thermal-mechanical analysis approach, the frames were assessed, and displacements and internal forces in the members were calculated. According to the results, in scenarios where fire occurs in the braced spans, structural stability is maintained for a longer duration, and the combination of braces and link beams significantly influences the redistribution of applied loads to adjacent columns [27].

This study evaluates two examples of three- and nine-story steel moment-resisting frames under fire conditions. Various fire scenarios were considered for each frame, and the frames were modeled in OpenSees [28] for simulated fires, with their performance analyzed in each scenario. For every scenario, the deflection of the mid-span beams, demand to capacity ratio (DCR) of beams and columns, and drift to allowable drift ratio of all stories were examined. Ultimately, the critical scenario for each frame was determind. In this study, the excessive deflection rates and deflections in the beams due to fire were calculated and compared according to the standards BS-476 [29] and ASTM E119 [30]. Fire duration of 120 minutes with a fire temperature of 1050 °C was considered for each scenario. The findings emphasize the need for enhanced fire-resistant design strategies to improve the safety and performance of steel

moment-resisting frames under fire conditions. By identifying critical scenarios and vulnerable structural members, engineers can develop more robust designs that enhance the safety and resilience of buildings under fire conditions.

2. Fire exposure conditions

In recent years, fire safety has become a critical factor in the design of new buildings and existing structures. With the increase in urbanization and the construction of high-rise buildings, the risk of fire hazards has risen, making fire protection a top priority in architecture and engineering. Fires pose a significant risk to steel structures, as high temperatures can considerably alter the mechanical properties of steel. As the temperature increases, steel loses its strength and stiffness, and a rapid decline in resistance is observed at temperatures exceeding 600 °C. This phenomenon may lead to instability and even structural collapse. At temperatures above 400 °C, the yield strength of steel decreases sharply, reaching its maximum reduction between 700 and 800 °C [31]. At elevated temperatures, steel exhibits increased deformation and may experience buckling or bending. Furthermore, the thermal expansion of steel can generate additional stresses in connections and other structural components. In general, structures may experience thermal and mechanical changes in fire conditions that require careful analysis and effective simulations.

2.1. Time-temperature curve

One of the methods for designing and evaluating a building's fire resistance is the use of published fire curves. These curves include the standard fire curve, the external fire curve, and the hydrocarbon fire curve. The time-temperature curve for a fire is a graphical representation of the changes in temperature over time, from the moment of ignition to the point at which the fire reaches its maximum intensity and then begins to decline. During this process, the temperature rises continuously until it reaches a very high level, which is usually associated with flashover or full fire involvement of the combustible materials in the environment. Figure 1 illustrates a typical time-temperature curve for the complete fire development process in a standard room, assuming no fire suppression measures are applied [31].

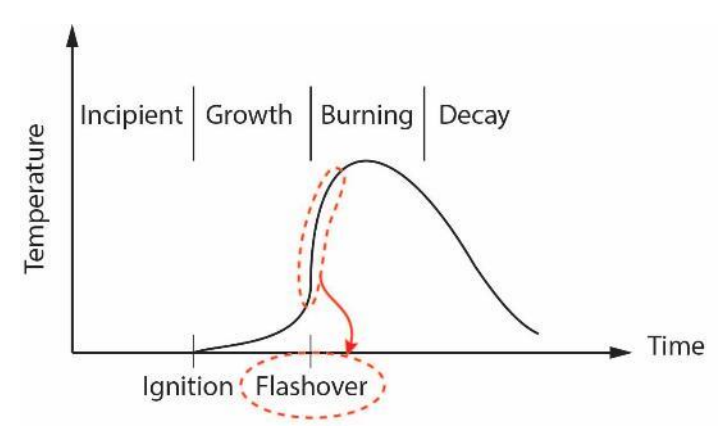


Fig. 1. Time-temperature curve for the complete fire development process.

Estimating temperatures during post-flashover fires is a critical aspect of fire safety design for structures. In such scenarios, temperatures typically reach around 1000 °C. The specific temperature at any given moment is determined by the equilibrium between the heat generated inside the enclosed space and the total heat lost to the surroundings [31]. Standard curves, often used in various engineering and safety applications, represent predefined or expected behaviors of systems under certain conditions. They are used to model phenomena in a way that allows for better prediction, analysis, and comparison. In fire safety standard fire curves are used to simulate the growth and behavior of fires over time. These curves help engineers design fire protection systems by providing a predictable fire temperature rise, which is

crucial for determining material resistance, fireproofing methods, and emergency planning. Designers can predict potential risks, incorporate necessary precautions and make the systems safer and more efficient using the curves. Standard fire curves, established by international organizations such as ISO, are recognized as tools for simulating fire behavior under standardized conditions. These curves are specifically designed to illustrate how temperature changes over time and it is usually assumed that the fire increases at a specified rate. The role of these curves in fire engineering and building safety is of significant importance. They are used for designing fire suppression systems, assessing the fire resistance of buildings, and analyzing the performance of construction materials under high temperatures. Particularly, the ISO-834 [32] standard fire curve, recognized as one of the most crucial standards, reflects the critical fire loading conditions in buildings and examines the behavior of structures under these conditions. Figure 2 shows the time-temperature curve of the ISO-834 fire after the flashover stage, where the temperature increases with time. This stage is one of the critical points of a fire that can have significant effects on the structure. The time-temperature equation for the ISO-834 standard curve is also defined according to Eq. 1 [32]:

$$T_{g} = 20 + 345\log(8t + 1) \tag{1}$$

where, T_g is the gas temperature, t is the time in minutes.

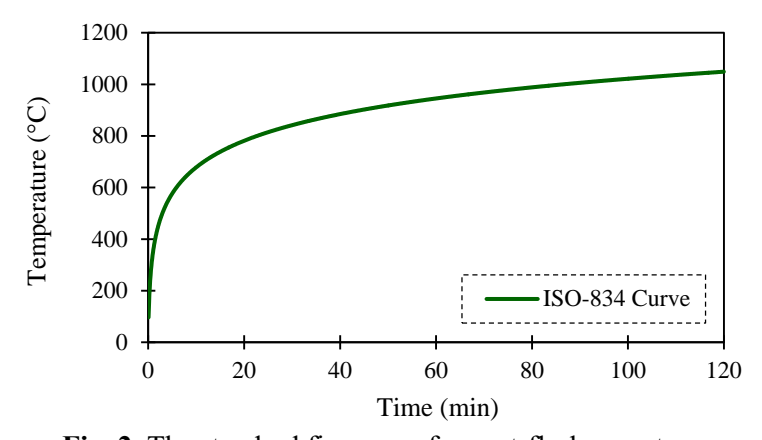


Fig. 2. The standard fire curve for post-flashover stage.

2.2. Heat transfer calculations

Heat transfer in fires is critical for understanding how fire affects structures, especially steel. There are three common modes of heat transfer in fire scenarios: conduction, convection, and radiation. In conduction, heat is transferred from one point of the object to another. In structures, conductive heat transfer can occur through structural materials such as steel and concrete, with steel occurring more rapidly. Calculations of conduction require determining the parameters of density, specific heat capacity, and heat transfer coefficient according to fire standards [33]. The rate of heat transfer in conduction can be calculated as [33]:

$$q = -kA \frac{\partial T}{\partial x} \tag{2}$$

where, q is the heat transferred, k is the conduction heat transfer coefficient and $A(\partial T/\partial x)$ is the temperature gradient in the direction of heat flow. In a steady-state condition, there is no need to consider the heat required to change the temperature of a material that is either heating or cooling.

Convection refers to the transfer of heat through a fluid from one point to another, or the transfer of heat from the hot gases produced by a fire to the parts of a building that come into contact with them. In a fire scenario, hot gases rise due to their lower density compared to the cooler surrounding air, transferring

heat to surfaces they encounter. This process significantly impacts the temperature distribution throughout a structure and can accelerate the degradation of materials exposed to the fire. The heat transferred through convection can be calculated as [33]:

$$q = hA\Delta T \tag{3}$$

where, h is the convective heat transfer coefficient, A is the surface area of the solid object in contact with the fluid and ΔT is the temperature difference between the surface of object and the contacting fluid. For standard fire conditions, the heat transfer coefficient for convection was considered to be 25 W/m²K. Radiation is an exceptionally important heat transfer mechanism in fires. Energy is transferred by electromagnetic waves, which can travel through a vacuum or transparent media. This process is essential for the transfer of heat from flames to fuel, smoke to building materials, and a burning building to nearby structures. The equation of radiation heat transfer from one surface to another is defined as [33]:

$$q = \varepsilon F_G \sigma A (T_1^4 - T_2^4) \tag{4}$$

where, ε is the resultant emissivity of the two surfaces, F_G is the geometric view factor between the two objects, σ is Stefan-Boltzmann constant, A is the exposed surface area of the object, T_I and T_2 are the temperatures of the objects. To protect a structure against fire, various methods are used, such as fireproof coatings and protective concrete. These materials are heat insulators and prevent the direct transfer of heat to the structural section. As a result, the temperature of the section increases more slowly, and its resistance is maintained for a longer period. This increases the evacuation time and reduces the damage caused by fire. Besides whether a section is protected or not, several other factors influence the amount of heat transferred from a fire to structural elements such as fire intensity and duration, material type and properties, section shape and dimensions and environmental conditions. The more intense the fire, the higher the ambient temperature and the greater amount of thermal energy released. Consequently, more heat is transferred to the structure. The longer the fire burns, the longer structural elements are exposed to high temperatures, resulting in greater heat absorption.

2.3. Temperature calculation for unprotected steel

In the Eurocode standard [34], formulas are provided for determining the temperature of both protected and unprotected steel sections, accounting for the effect of fire on different surfaces of the structural members. In this study, unprotected sections are considered for the members of the frames. The temperature of an unprotected steel member during a time step (Δt) in °C can be calculated as:

$$\theta_{i} = \theta_{i-1} + (\Delta \theta_{i}) \theta_{o} \tag{5}$$

where, θ_i is the temperature of the member at time step i, θ_{i-1} is the temperature at time step (i-1), θ_0 is the ambient temperature before the fire, $\Delta \theta_i$ is the temperature growth of the unprotected steel member during the time step (Δt) can be calculated by Eq. (6) [34].

$$\Delta \theta_{i} = k_{sh} \frac{\underline{A}_{m}}{C_{a} \rho_{a}} \dot{h}_{net,d} \Delta t \tag{6}$$

where, A_m is the surface area of the member per unit length, V is the volume of the steel member per unit length, (A_m/V) is the section factor of the steel member, Δt is the time interval should not be taken as more than 5 seconds [34], C_a is the specific heat of steel, ρ_a is the unit mass of steel, k_{sh} is the correction factor for the shadow effect, and $\dot{h}_{net,d}$ is the design value of the net heat flux per unit area can be calculated as:

$$\dot{h}_{net,d} = \dot{h}_{net,c} + \dot{h}_{net,r} \tag{7}$$

$$\dot{h}_{net,c} = \alpha_c \cdot (\theta_g - \theta_m) \tag{8}$$

$$\dot{h}_{net,r} = \varphi \cdot \varepsilon_m \cdot \varepsilon_f \cdot \sigma \left[(\theta_r + 273)^4 - (\theta_m + 273)^4 \right] \tag{9}$$

where, α_c is the convective heat transfer coefficient taken as 25 in this study, θ_g is the gas temperature in the vicinity of the fire exposed member, θ_m is the surface temperature of the steel member, θ_r is the effective radiation temperature for the fire environment, φ is the configuration factor taken as 1 in this study, ε_m is the surface emissivity of the steel taken as 0.8 in this study, ε_f is the emissivity of the fire taken as 1, and σ is the Stefan-Boltzmann constant (approximately $5.67 \times 10^{-8} \text{ W/m}^2 \text{K}^4$). Finally, the shadow effect factor (k_{sh}) is determined using Eqs. (10) and (11) for general and I-shaped sections.

$$k_{sh} = \left(\frac{A_m}{V}\right)_h / \left(\frac{A_m}{V}\right) \tag{10}$$

$$k_{sh} = 0.9 \times \left(\frac{A_m}{V}\right)_b / \left(\frac{A_m}{V}\right) \tag{11}$$

where, $(A_m/V)_b$ is the box value of the section factor.

3. Case studies

In this study, two dimensional three and nine-story steel moment frames [35] are modeled and analyzed under fire conditions using OpenSees software. In both examples, The yield strength of the steel used for the columns and beams is 345 and 248 MPa, respectively. Also, the expected yield strength of the columns and beams is 397 and 339 MPa, respectively. The modulus of elasticity and the specific weight of steel are 200 GPa and 7850 kN/m, respectively. The column sections were selected as wide-flange sections W8 to W14 and the beam section list was made by all W-shaped sections. For each frame, a constant gravity load of 28.7 kN/m (W_2) was distributed on the roof beams, while a constant gravity load of 32 kN/m (W_1) was applied to the first and second floors in the three-story and the first to eighth floors in the nine-story frame.

3.1. Three-story four-bay steel frame

In this study, a three-story steel frame with four spans was considered as the first example as shown in Fig. 3. Grouping of the elements and gravity loads of the frame are shown in Fig. 3. The length of each bay is 9.15 m, and the height of each story is 3.96 m. Figure 4 shows the element numbering of three-story steel frame. The sections of each group for the three-story frame are presented in Table 1 [35].

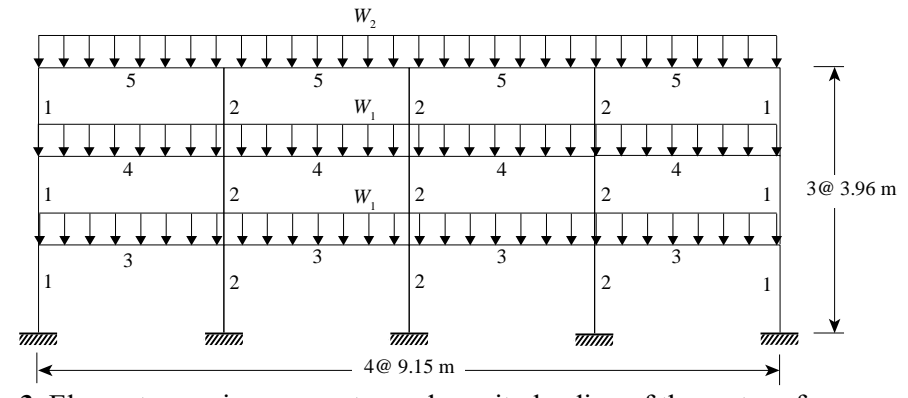


Fig. 3. Element grouping, geometry and gravity loading of three-story frame.

C1		C2	C3	C4	C5
]	B16	B17	B18	B19	
Cb		C/	C8	(5)	C10
	B20	B21	B22	B23	G10
			CIS		
C11		C12	C13	C14	C15
	B24	B25	B26	B27	
	C11	B20	C11 C12 B20 B21 C6 C7	C11 C12 C13 C13 C16 B20 C7 C8 C8	C11 C12 C13 C14 C14 C16 B20 C7 C8 C9 C9

Fig. 4. Element numbering of three-story frame.

Table 1. Sections of each group for three-story frame.

	<u> </u>
Grouping of elements	Section
1	W16 × 57
2	$W18 \times 71$
3	W24 ×55
4	$W18 \times 55$
5	$W16 \times 45$

3.2. Nine-story five-bay steel frame

A nine-story steel frame with five spans was considered as another example as shown in Fig. 5. Grouping of the elements and gravity loads of the frame are shown in Fig 5. The length of each bay was 9.15 m and the height of each story, except for the first story, was 3.96 m. The height of the first story was 5.48 m. Figure 6 shows the element numbering of nine-story frame. The sections of each group for nine-story frame are shown in Table 2 [35].

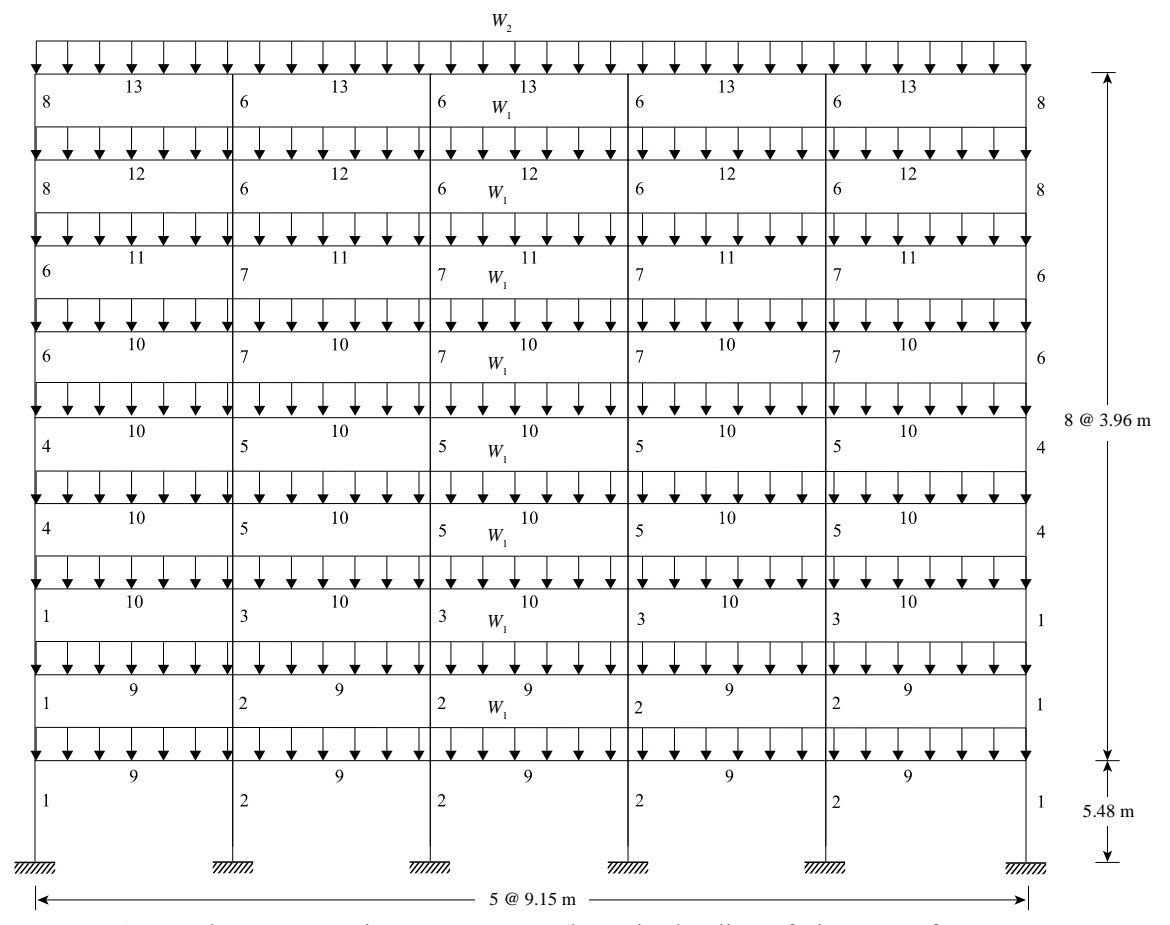


Fig. 5. Element grouping, geometry and gravity loading of nine-story frame.

B95	B96	B97	B98	B99	
C49	C50	C51	C52	C53	C54
B90	B91 C44	B92 C45	B93	B94	C48
C43	C44	C45	C46	C47	C46
B85	B86	B87	B88	B89	C42
C37	C38	C39	C40	C41	C42
B80	B81	B82	B83	B84	624
C31	C32	C33	C34	C35	C36
B75	B76	B77	B78	B79	
C25	C26	C27	C28	C29	C30
B70	B71	B72	B73	B74	
C19	C20	C21	C22	C23	C24
B65	B66	B67	B68	B69	
C13	C14	C15	C16	C17	C18
B60	B61	B62	B63	B64	
C7	C8	C9	C10	C11	C12
B55	B56	B57	B58	B59	
C1	C2	C3	C4	C5	C6
<i>////</i> ,	<i>1111111</i> ,	<i>,,,,,,,,</i>	<i>''''''</i> '''	<i>,,,,,,,,</i>	7//////

Fig. 6. Element numbering of nine-story frame.

Table 2. Sections of each group for nine-story frame.

Grouping of elements	Section
G1	W14 × 211
G2	$W14 \times 159$
G3	W14 ×159
G4	$W14 \times 90$
G5	$W14 \times 145$
G6	$W14 \times 82$
G7	$W14 \times 109$
G8	$W14 \times 68$
G9	$W30 \times 99$
G10	$W24 \times 84$
G11	$W16 \times 67$
G12	$W18 \times 55$
G13	$W12 \times 50$

3.3. Fire scenarios

In two examples, several fire scenarios in various floors and spans have been examined. The goal of analyzing the frames with different fire scenarios is to investigate inter-story drift, deflection of beams, and demand-to-capacity ratio of stress for the beams and columns to determine the most critical scenarios. In fact, the objective of this study is to investigate the critical scenarios that lead to a rapid structural collapse, especially focusing on where the occurrence and initiation of a fire in the structure can lead to a quicker total collapse. A fire duration of 120 minutes at a temperature of 1050 °C was assumed for each scenario. Figure 7 shows the different fire scenarios for three-story frame. The time-temperature curves of the beams and columns exposed to fire were calculated based on the Eqs. (5) to (11).

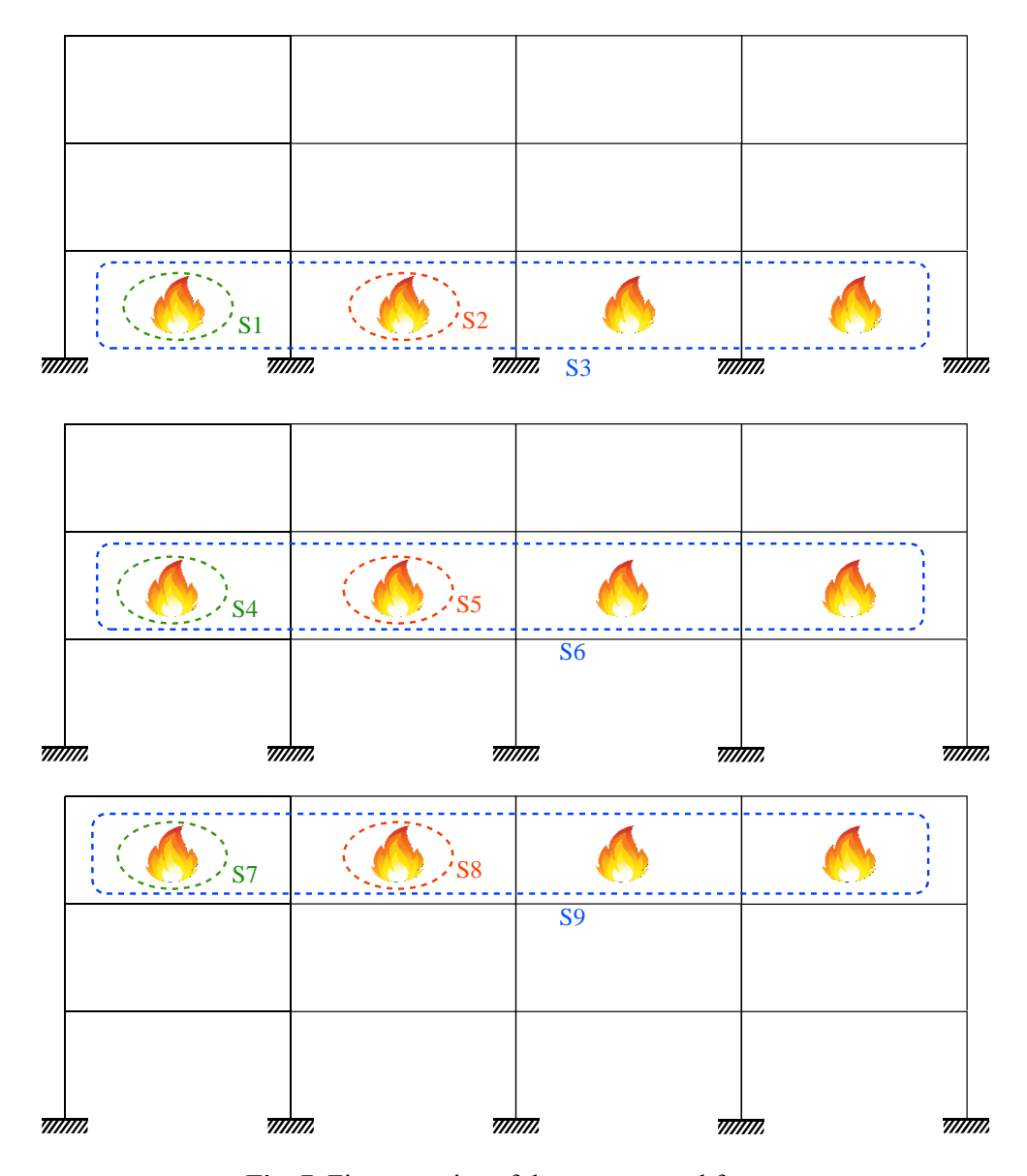


Fig. 7. Fire scenarios of three-story steel frame.

Figure 8 indicates the time-temperature curves of elements under fire for three-story steel frame. The members within a group share common characteristics, reflecting a unified pattern of behavior or properties. Therefore, the fire curves are presented according to the grouping number of the elements for each scenario.

Figure 9 shows the fire scenarios for nine-story frame. The time-temperature curves of elements under fire for nine-story steel frame are shown in Fig. 10. Figure 11 indicates the flowchart of the thermal analyses prossess. According to the flowchart, the static analysis of frames was conducted under gravity loads. Next, the temperatures from the ISO-834 time-temperature curve during the fire stages were extracted. According to the flowchart, heat transfer calculations can be used to transfer the ambient temperature to the component. Based on whether the section is protected or unprotected, the relevant equations for each condition must be applied. Therefor, heat transfer calculations were performed to implement the heat transfer analysis and then the thermal analysis of the frames was conducted using OpenSees [28]. In fact, this stage determines the amount of heat transfer from the fire to the structural elements. The amount of heat transfer is different for the protected and unprotected sections. If the section is protected, less heat is transferred to it, and the section will be damaged over a longer time. Ultimately, after comparing the results of analyses, critical scenarios can be determind.

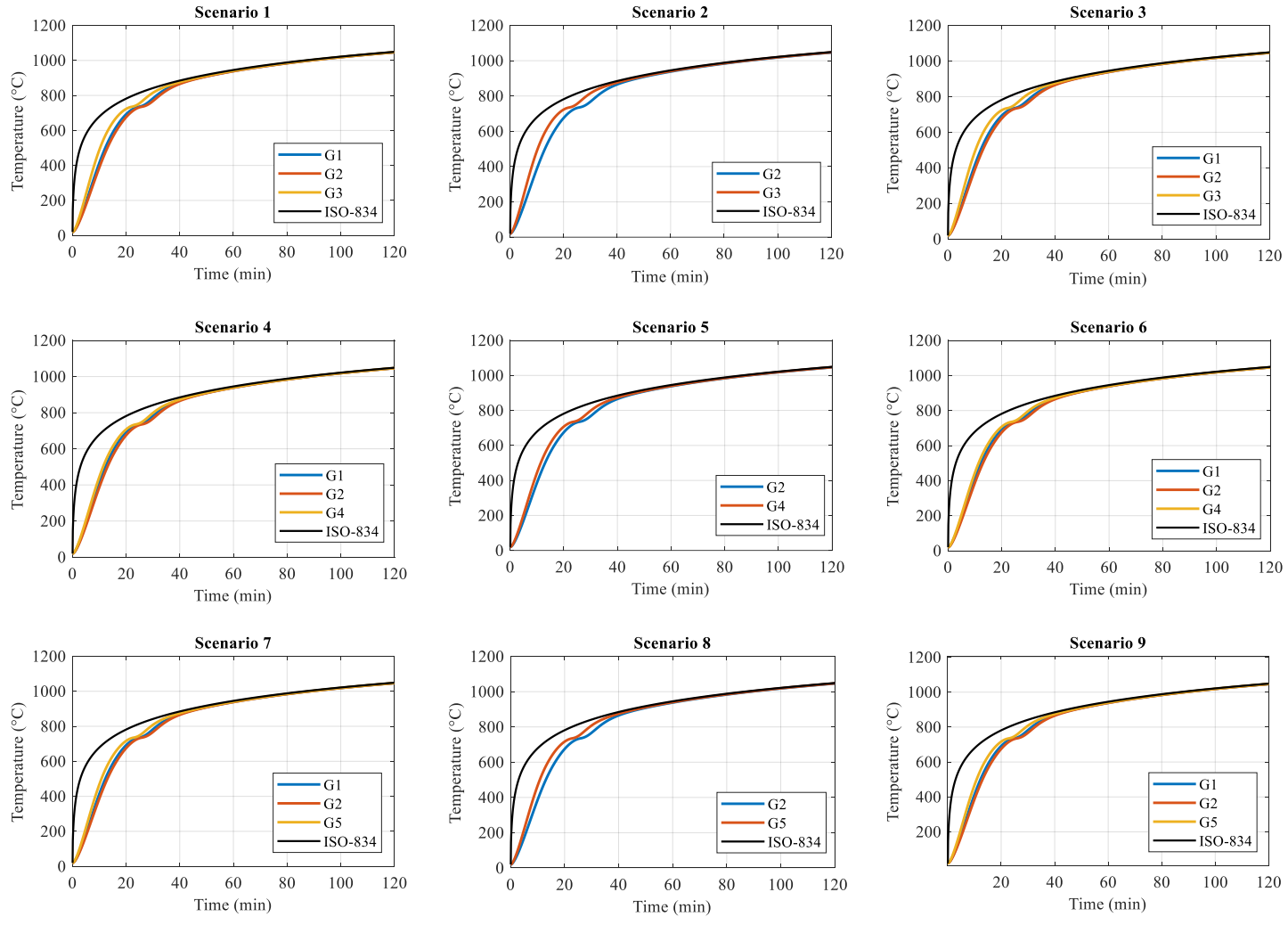


Fig. 8. Time-temperature curves of element grouping under fire for three-story frame.

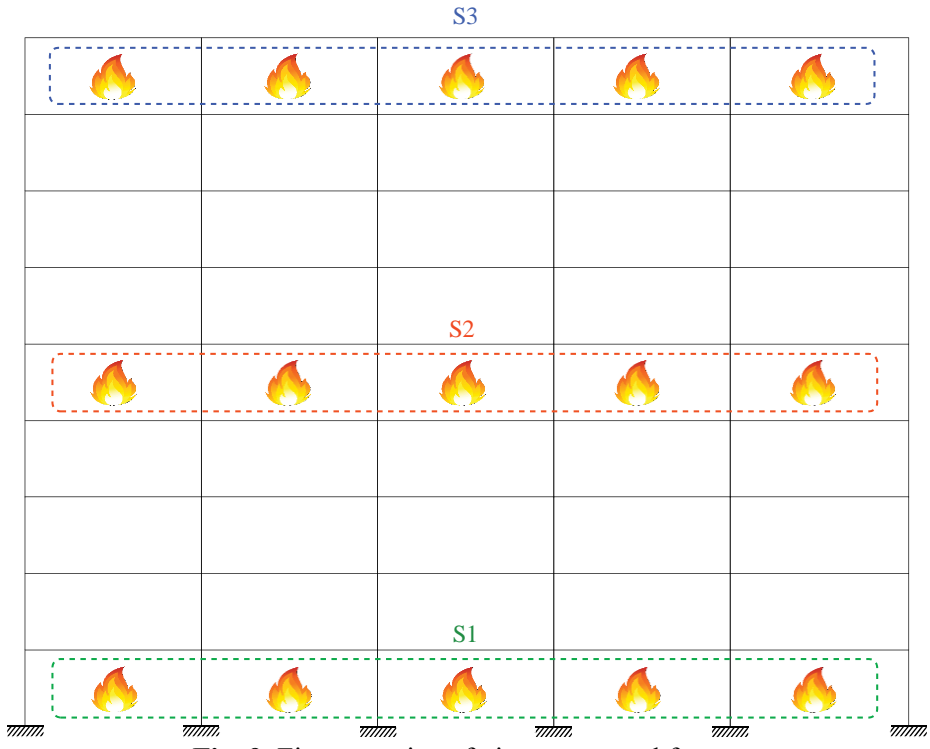


Fig. 9. Fire scenarios of nine-story steel frame.

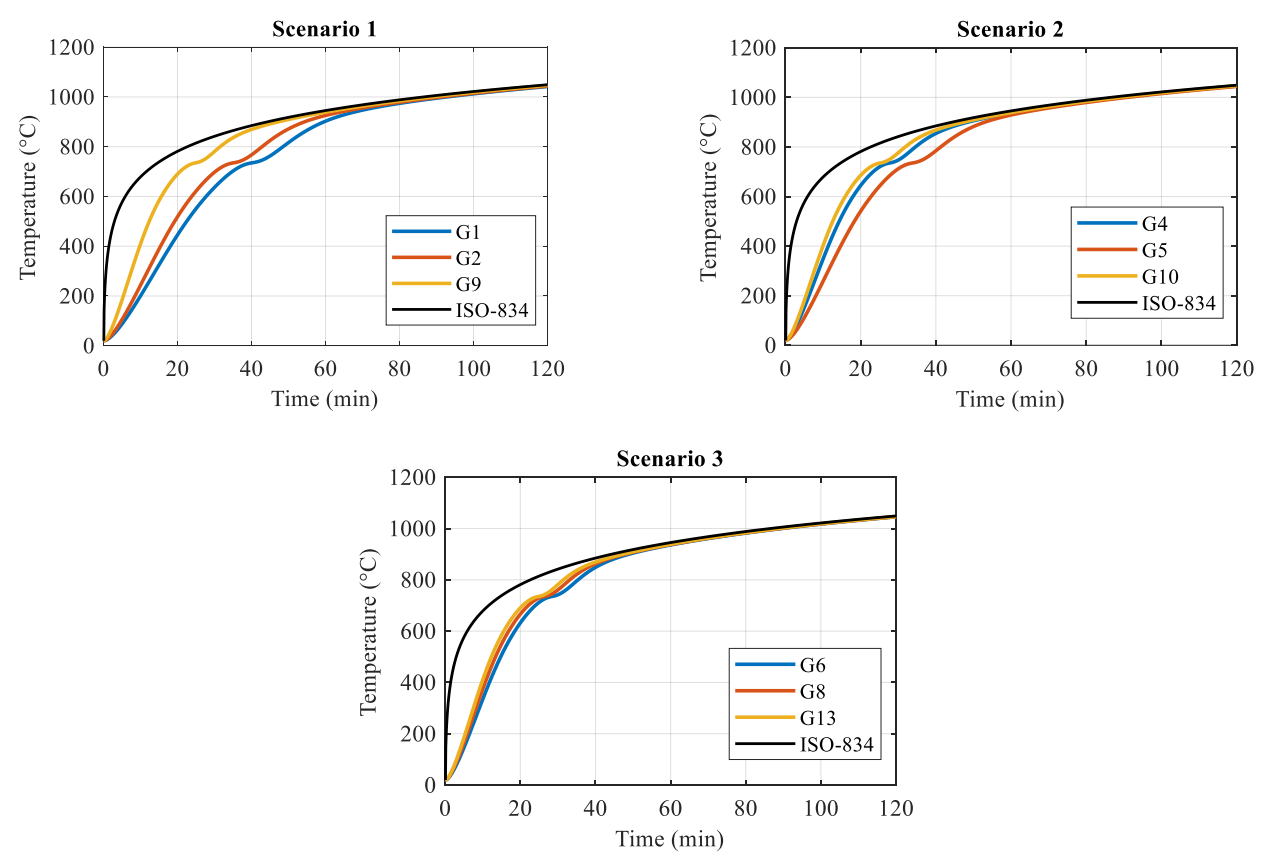


Fig. 10. Time-temperature curves of element grouping under fire for nine-story frame.

3.4. Key findings, strengths, limitations and practical applications

This study identified critical fire scenarios for each frame, which can significantly contribute to improving fire-resistant design methods and investigated the behavior of three- and nine-story steel frames under fire conditions. The study has several strengths, such as a comprehensive analysis of multiple fire scenarios and the identification of critical failure points, including vulnerable columns and lower-to-mid-level stories. The identification of critical scenarios for each structure is a notable strength, as this information can significantly contribute to the design of more fire-resistant structures. However, the study has certain limitations. For instance, it employs a fixed fire temperature (1050°C) and duration (120 minutes), which may not fully capture real-world variability. Additionally, the research focuses on traditional steel structures and does not explore advanced materials or composites with enhanced fire resistance. Furthermore, the dynamic effects of fire, such as explosions or sudden temperature changes, have not been considered, even though these factors can substantially influence structural behavior.

4. Results of fire scenarios

In this study, the performance criteria have been used to control the beams failure according to BS-476 [29] or ASTM E119 [30]. The deflection and deflection rate of beams in fire conditions are investigated based on the standards. According to the standards, beam failure occurs when any of the requirements is specified:

- (I) The beam deflection is greater than L/20 (according to BS-476) or $L^2/400d$ (according to ASTM E119)
- (II) The beam deflection is greater than L/30 and the beam deflection rate is also greater than $L^2/9000d$ (according to BS-476)

where, L is the beam span length and d is the beam depth. The deflection rate is the ratio of deflection changes to time changes.

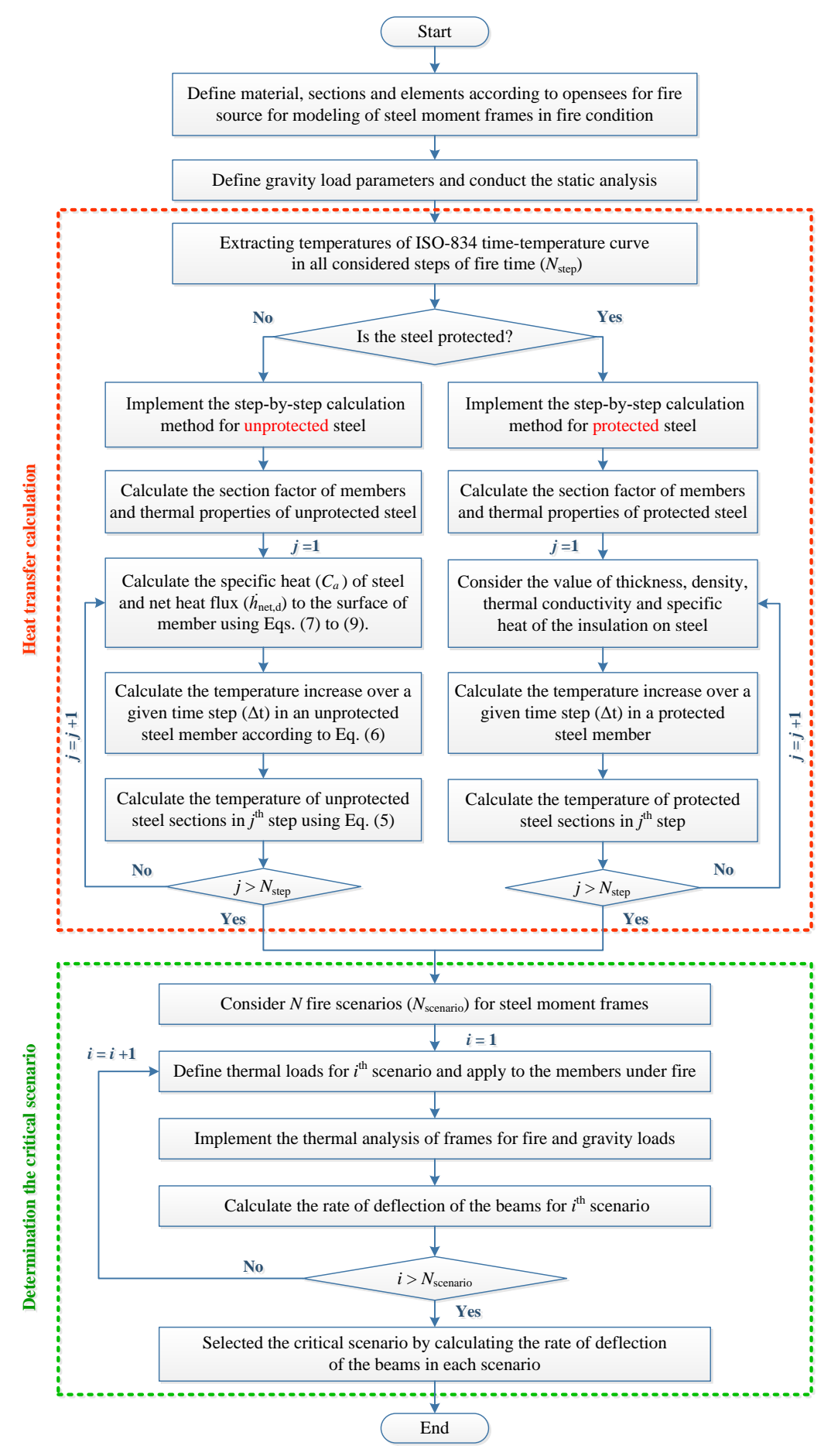


Fig. 11. The flowchart of the thermal analyses prossess.

The values of the failure criterion of beams in three- and nine-story frames according to BS-476 and ASTM E119 are listed in Table 3. The values of mid-span deflection, deflection rate, time, and temperature of the beams under fire exposure at the time of structural failure for three- and nine-story frames are presented in Tables 4 and 5, respectively. The variation of mid-span deflection with temperature and time of only beams under fire exposure for three-story frame is shown in Fig. 12.

Table 3. Failure criteria of the beams under fire in three- and nine-story frames based on BS-476 and ASTM E119.

	Member dimensions		ASTM E119 failure criteria		BS-476 failure criteria		
		_	(1)	(2)	(1)		(2)
Member section	d	L	$L^{2}/400d$	$L^2/9000d$	L/20	L/30	$L^2/9000d$
Member section	(mm)	(mm)	(mm)	(mm/min)	(mm)	(mm)	(mm/min)
W24 × 55	599.44	9150	349.17	15.52	457.5	305	15.52
$W18 \times 55$	459.74	9150	455.27	20.23	457.5	305	20.23
$W16 \times 45$	408.94	9150	511.82	22.75	457.5	305	22.75
$W30 \times 99$	754.38	9150	277.45	12.33	457.5	305	12.33
$W16 \times 67$	612.14	9150	341.92	15.19	457.5	305	15.19
$W12 \times 50$	309.88	9150	675.44	30.02	457.5	305	30.02

Table 4. Deflection, rate of deflection, time and temperature of beams at the time of three-story frame failure.

	Beam	Deflection rate	Failure	Beam mid span	Time	Beam bottom flange
Scenario	number	(mm/min)	criterion	deflection (mm)	(min)	temperature (°C)
S1	B16	36.34	(II)	233.40	98	1016.34
S2	B17	20.641	(II)	207.37	88.41	1000.58
	B16	5.26	(I)	81.05		
S3	B17	16.20	(II)	208.58	87.41	998.84
33	B18	16.16	(II)	208.58	07.41	990.84
	B19	5.26	(I)	81.05		
S4	B20	36.34	(II)	293.58	98.67	1017.38
S5	B21	23.88	(II)	197.46	85.33	995.14
	B20	3.85	(I)	64.56		
S 6	B21	21.20	(II)	197.84	84.33	993.32
50	B22	21.26	(II)	197.90	04.55	773.32
	B23	3.82	(I)	64.56		
S7	B24	71.53	(II)	302.56	87.83	999.57
S8	B25	79.41	(II)	239.51	79.67	984.57
	B24	17.52	(I)	144.59		
S9	B25	22.26	(I)	214.04	82.83	990.57
39	B26	22.24	(I)	213.42	04.83	990.37
	B27	17.41	(I)	144.59		

Table 5. Deflection, rate of deflection, time and temperature of beams at the time of nine-story frame failure.

Scenario Beam		Deflection rate	Failure	Beam mid span	Time	Beam bottom flange
Sectiano Dear	Deam	(mm/min)	criterion	deflection (mm)	(min)	temperature (°C)
	B55	1.22	(I)	47.26		
	B56	1.76	(I)	84.58		
S1	B57	1.84	(I)	84.98	120	1046.54
	B58	1.76	(I)	84.58		
	B59	1.22	(I)	47.26		
	B75	1.83	(I)	45.43		
	B76	2.57	(I)	130.04		
S2	B77	2.84	(I)	164.84	120	1046.54
	B78	2.56	(I)	130.04		
	B79	1.83	(I)	45.43		
	B95	8.47	(I)	110.30		
]	B96	20.63	(I)	358.03		
S3	B97	50.47	(II)	551.22	80.42	984.81
	B98	20.63	(I)	358.05		
	B99	9.11	(I)	110.32		

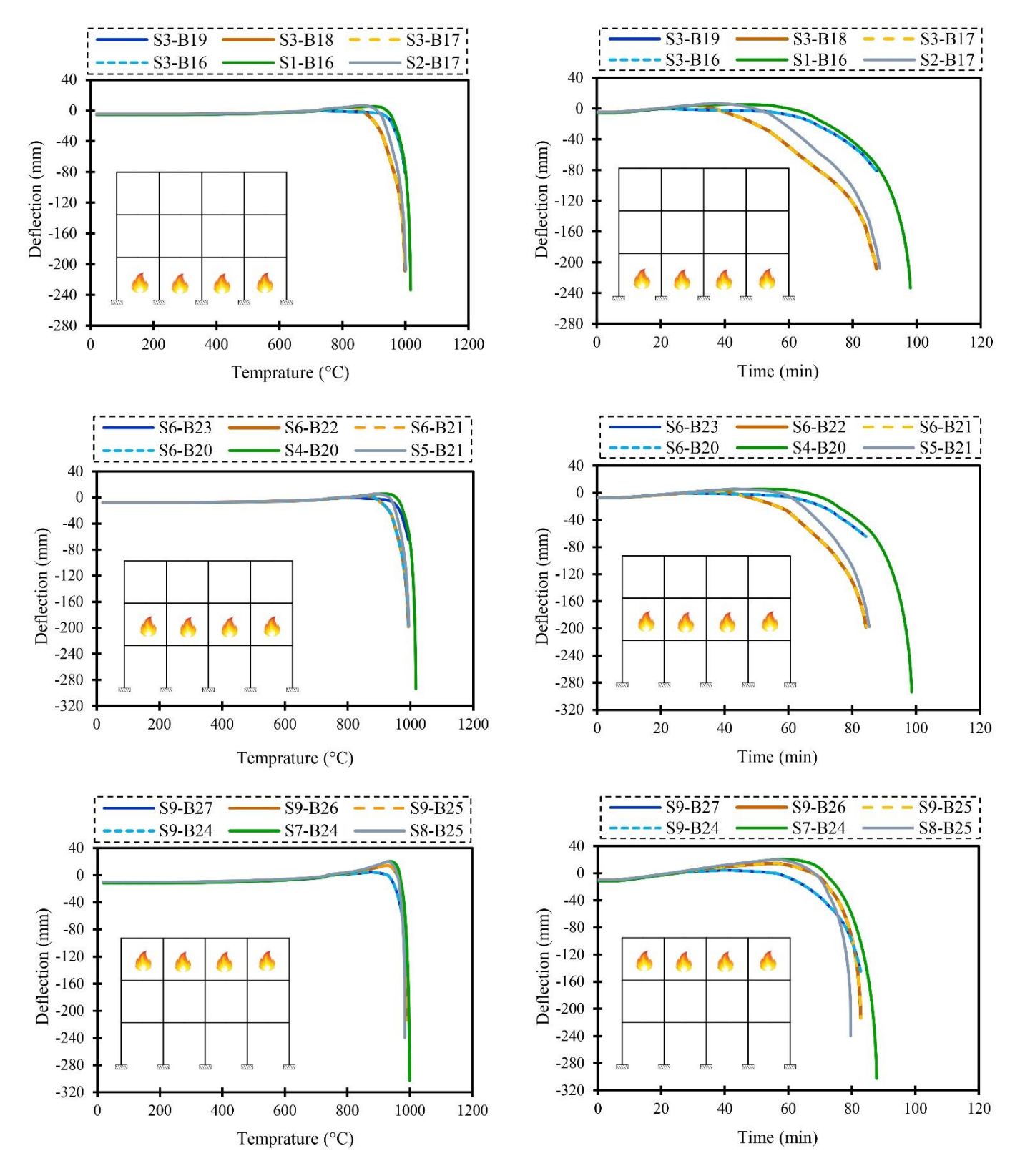


Fig. 12. Mid-span deflection versus time and temperature of the beams under fire scenarios for three-story frame.

The deflection values of beams in each story of the three-story frame were compared, and the critical scenario for each story was identified based on the beam that failed the fastest. Finaly, The critical scenario for the three-story frame was selected by comparing critical scenario in each story is shown in Fig. 13. Figure 14 indicates the deformation of frame and DCR range of elements in each scenario for three-story frame at the time of structural failure.

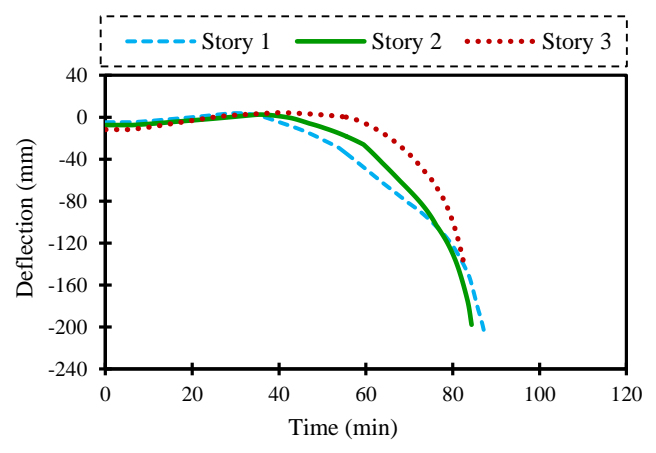


Fig. 13. Comparison the critical scenarios of each story in three-story steel frame.

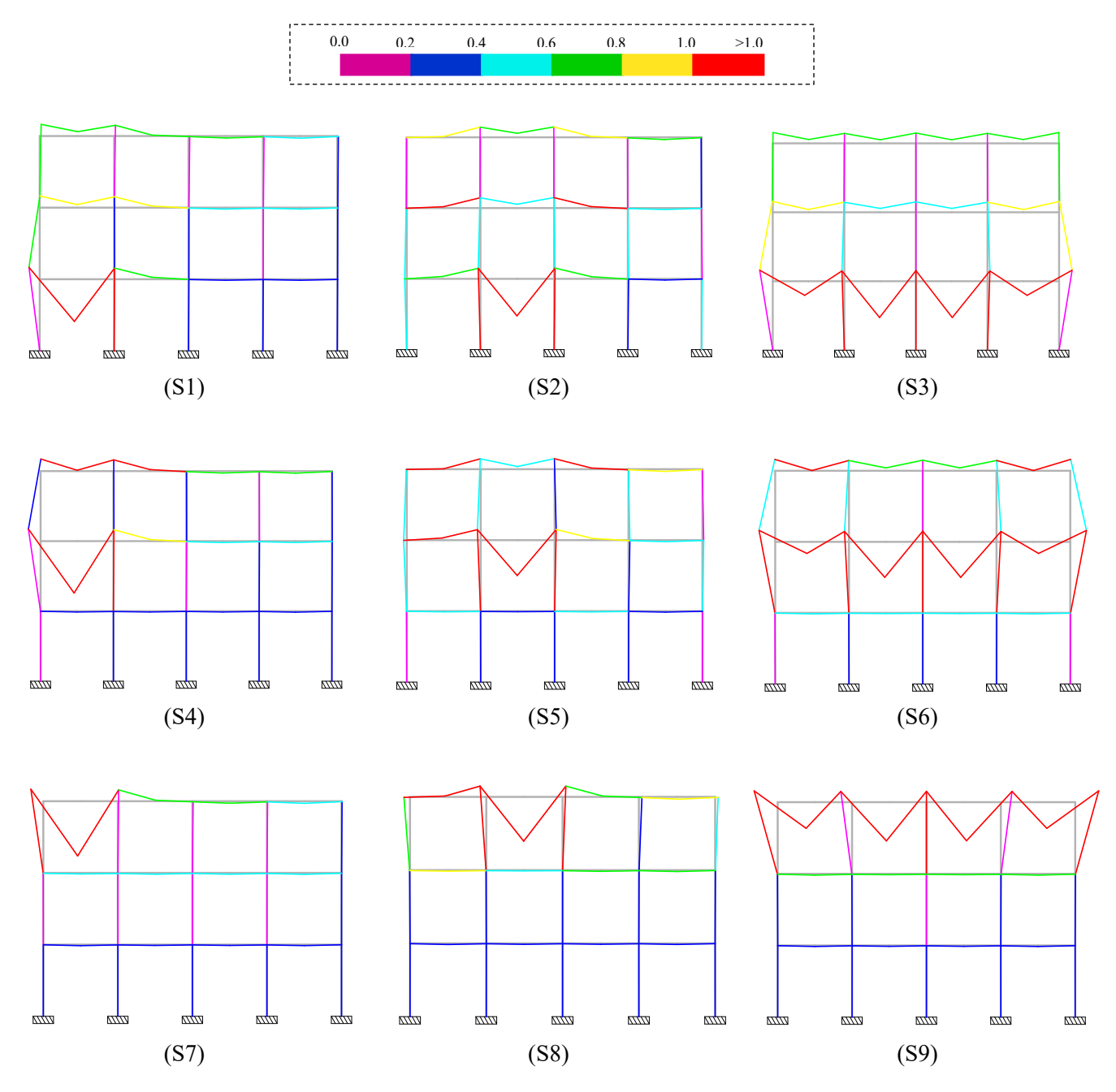


Fig. 14. Deformation and DCR range of the elements in each scenario for three-story steel frame.

The results were used to calculate the DCR and the capacity of the members and the critical scenarios were examined. In each scenario, thermal analysis was performed to calculate DCR of elements. Subsequently, the design criteria and evaluation standards for steel frame members under fire conditions will be provided according to Appendix 4 of the AISC specification 360-16 [36]. The appendix provides criteria for the evaluation of the steel frames in fire conditions. In this section, the DCR of heated elements at elevated temperatures under fire exposure is calculated as:

If
$$\frac{P_u(T)}{P_{cr}(T)} \ge 0.2$$
, $DCR(T) = \frac{P_u(T)}{P_{cr}(T)} + \frac{8}{9} \left(\frac{M_u(T)}{M_u(T)} \right)$ (12)

If
$$\frac{P_u(T)}{P_{cr}(T)} < 0.2$$
, $DCR(T) = \frac{P_u(T)}{2P_{cr}(T)} + \left(\frac{M_u(T)}{M_n(T)}\right)$ (13)

where, $P_{\rm u}(T)$ and $M_{\rm u}(T)$ are the required axial force and bending moment of elements at elevated temperatures, respectively. $P_{\rm cr}(T)$ and $M_{\rm n}(T)$ are the reduced axial strength and flexural strength of heated elements at elevated temperatures according to AISC 360-16, respectively. The demand to capacity ratio of the members at ambient temperature can be calculated as:

If
$$\frac{P_u(T)}{P_{cr}(20^{\circ}\text{C})} \ge 0.2$$
, $DCR(T) = \frac{P_u(T)}{P_{cr}(20^{\circ}\text{C})} + \frac{8}{9} \left(\frac{M_u(T)}{M_n(20^{\circ}\text{C})}\right)$ (14)

If
$$\frac{P_u(T)}{P_{cr}(20^{\circ}\text{C})} < 0.2$$
, $DCR(T) = \frac{P_u(T)}{2P_{cr}(20^{\circ}\text{C})} + \left(\frac{M_u(T)}{M_n(20^{\circ}\text{C})}\right)$ (15)

where, $P_{cr}(20^{\circ}\text{C})$ and $M_{n}(20^{\circ}\text{C})$ are the axial strength and moment strength of elements at ambient temperatures, respectively.

The values of DCR for the member actions versus time under different fire scenarios are shown in Fig. 15. For example, the DCR of the heated elements in scenarios 2, 7 and 8 for three-story frame is shown in Fig. 16. In this study, story drift for fire condition was also investigated. The values of inter-story drift to allowable drift ratio of the stories in each scenario for three-story frame are shown in Fig. 17. The allowable inter-story drift of structure is considered based on AISC specification 360-16.

The results of scenarios 1, 2, and 3 in three-story frame show that the critical condition, based on the beam deflection, occurs in fire scenario 3 in the first story. Also, the critical condition for the second and third story based on the beam deflection are scenarios 6 and 9, respectively. Based on the comparison of the results from the selected scenarios for each floor, it can be concluded that the critical scenario, in terms of beam failure in the three-story frame, is the first story. This is because the critical beam on the first story tends to fail in a shorter time compared to the beams on other floors. Additionally, the demandto-capacity ratio values of the members, as shown in Fig. 15, indicate that the DCR values for the members in scenarios 1, 2, and 3 (which correspond to the first story) exceed the allowable limit of 1.0 in a shorter time. The columns experience the highest DCR values in the shortest time, further emphasizing that the first story is more critical compared to the other stories in the three-story frame. Furthermore, as illustrated in Fig. 17, the drift to allowable drift ratio in scenarios 1, 2, and 3 is significantly higher than other scenarios. The results indecate that occurrence of fire in the first story not only induces significant displacement on the first story but also propagates substantial displacement to the upper levels, thereby creating a more critical and widespread risk of structural collapse. According to the results the first story is particularly vulnerable because its structural members, especially the columns, fail in a faster time than other stories.

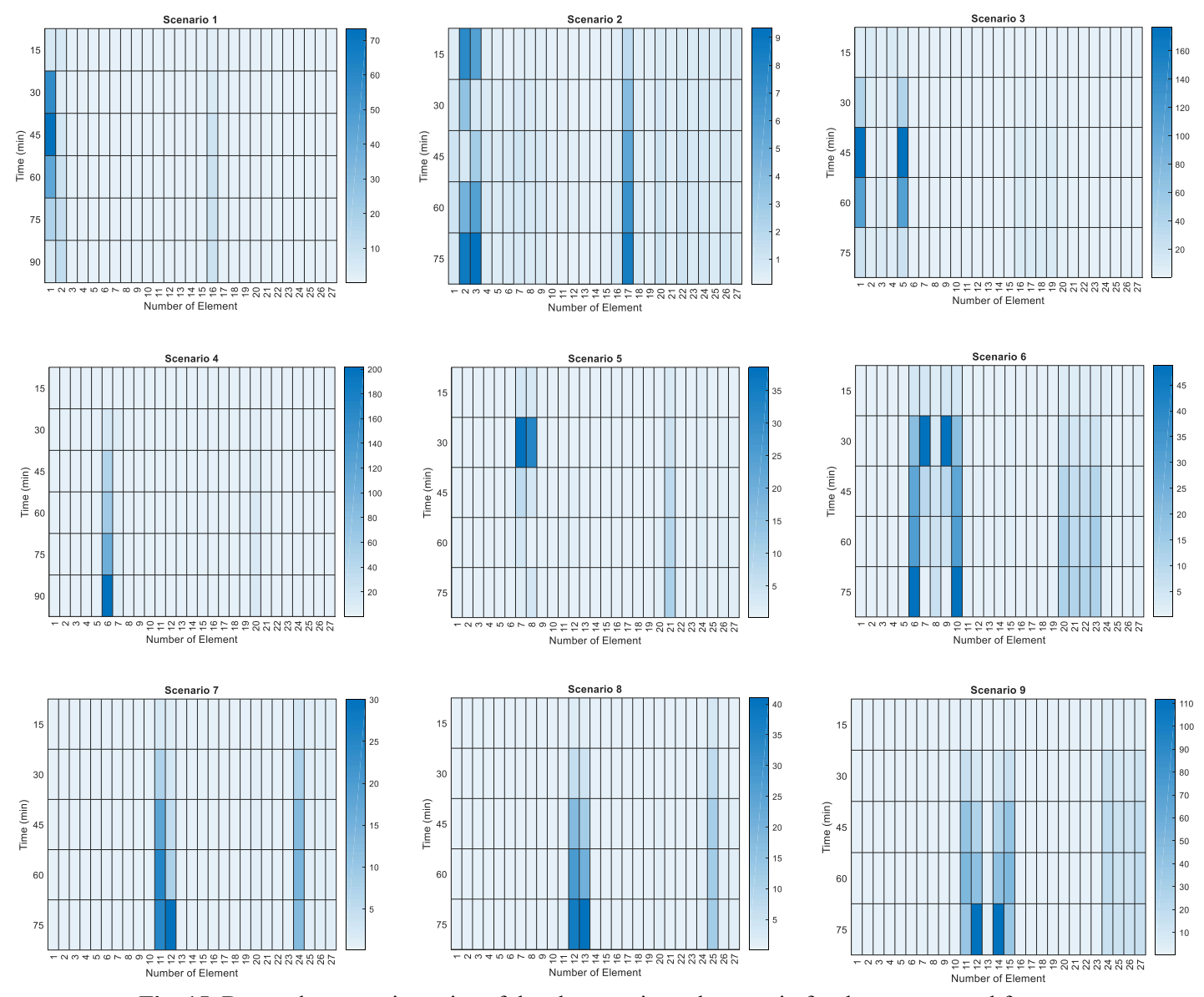


Fig. 15. Demand to capacity ratios of the elements in each scenario for three-story steel frame.

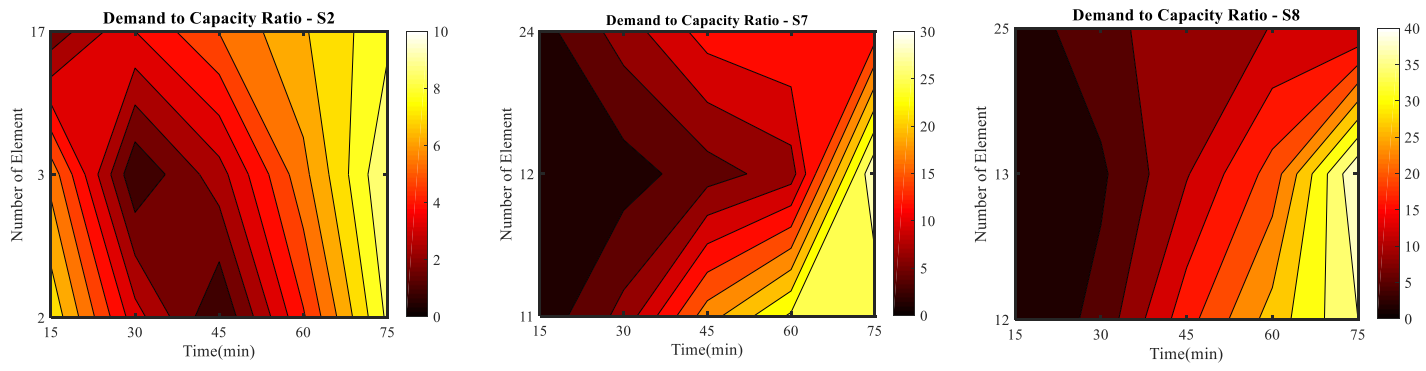


Fig. 16. DCR of the elements in scenarios 2, 7 and 8 for three-story steel frame.

The variation of beam deflection with temperature and time in fire conditions for nine-story frame is shown in Fig. 18. By comparing the deflection values of beams in each story under fire for the nine-story frame, the critical deflection values were determined according to the beam that experienced failure in the shortest time as shown in Fig. 19.

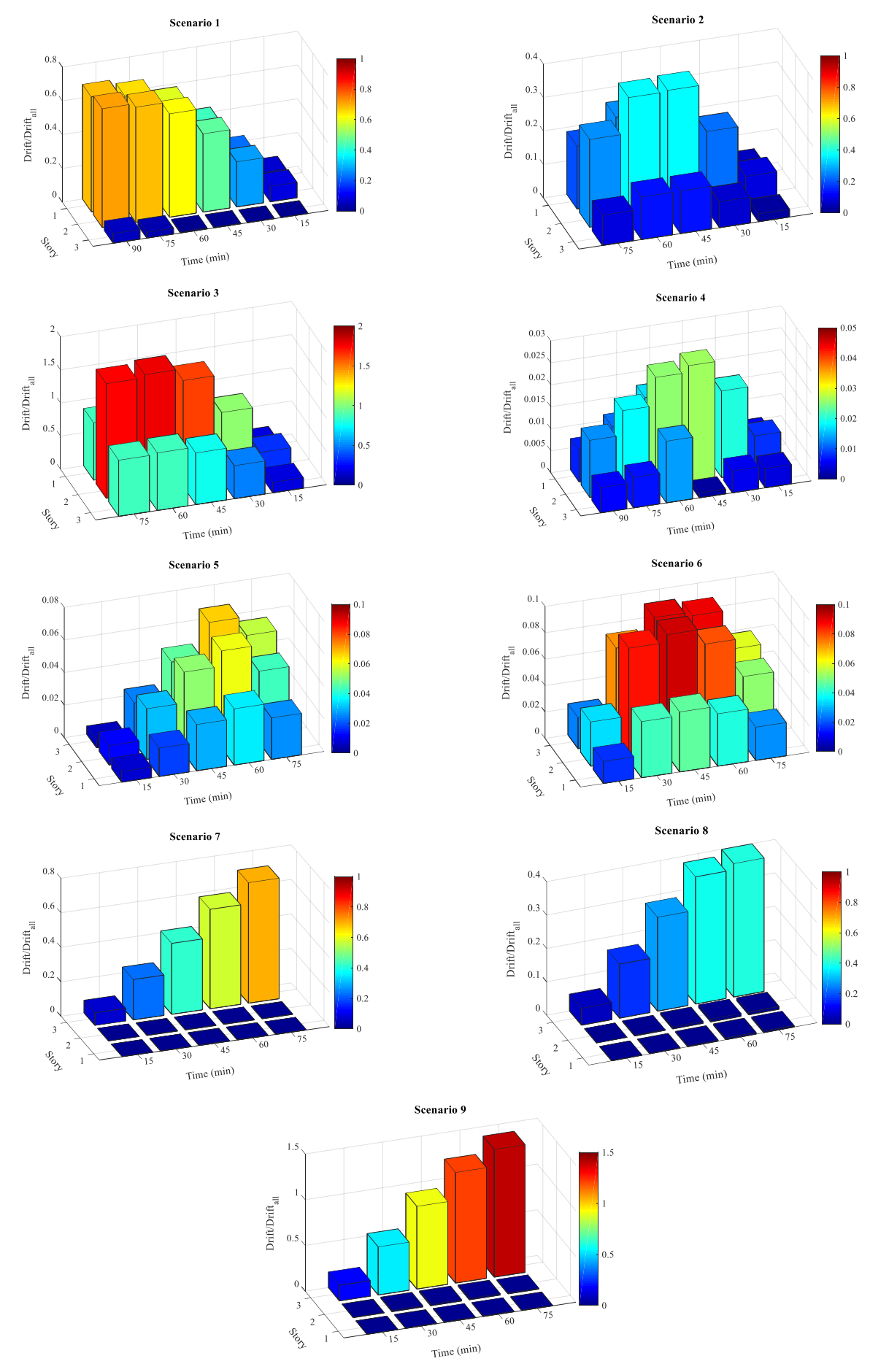


Fig. 17. Drift to allowable drift ratio of the stories in each scenario for three-story steel frame.

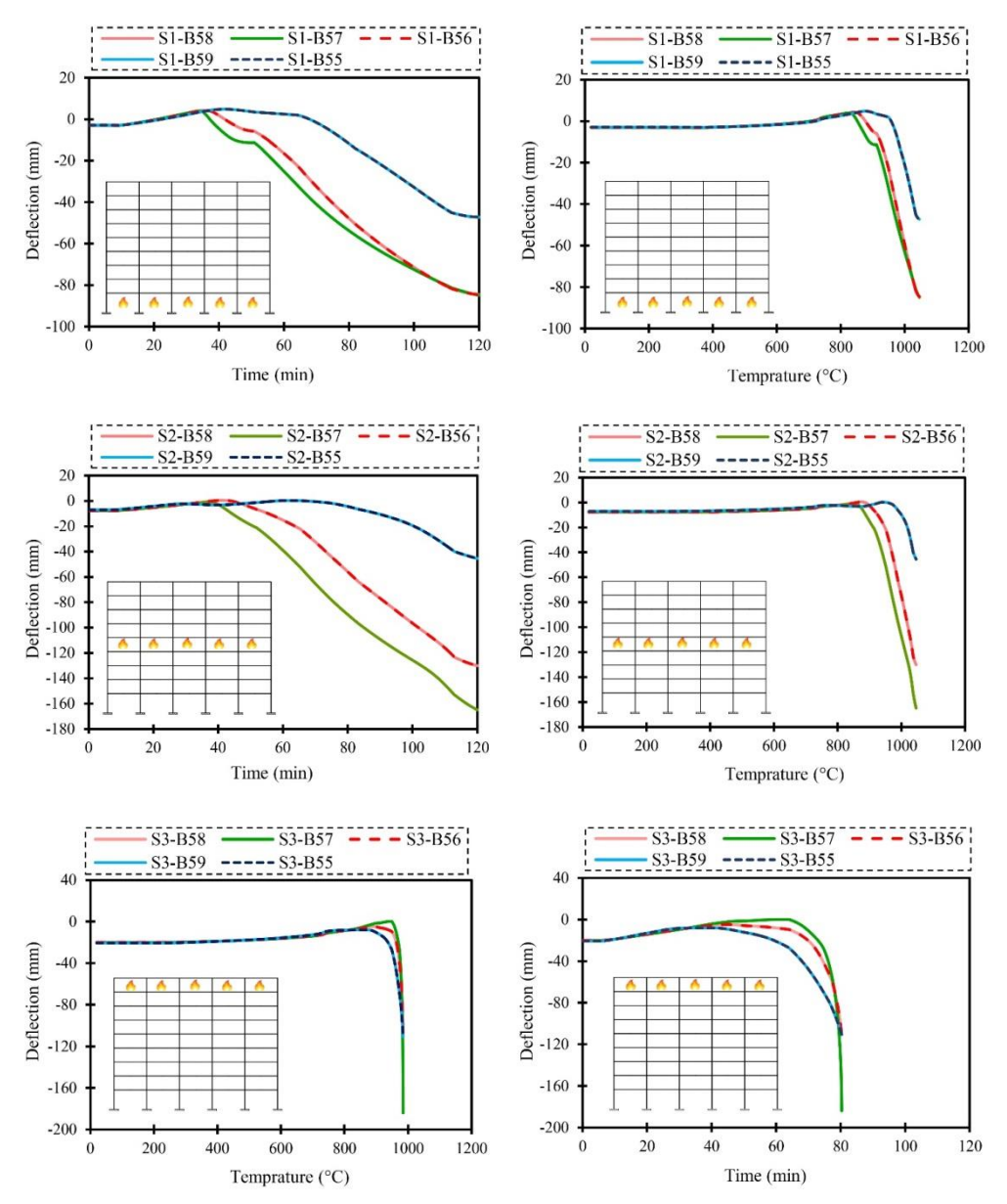


Fig. 18. Mid-span deflection versus time and temperature of the beams under fire scenarios for nine-story frame.

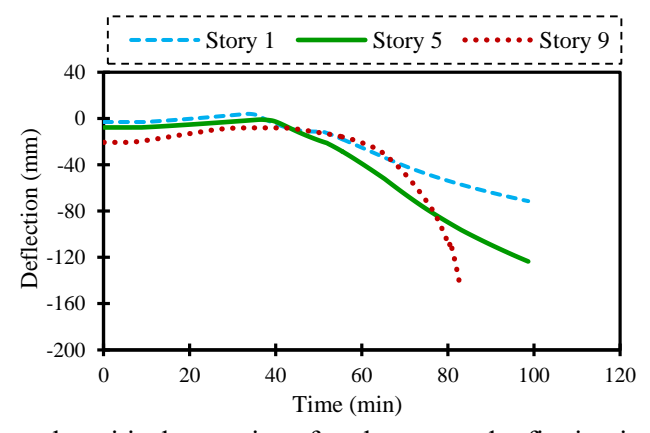


Fig. 19. Comparison the critical scenarios of each story under fire in nine-story steel frame.

Figure 20 indicates the deformation of frame and element DCR range in each scenario for nine-story frame at the time of structural failure. The values of DCR for the actions of the structural members at each scenario are shown in Fig. 21. The values of drift to allowable drift ratio of the stories in each scenario for nine-story frame are shown in Fig. 22.

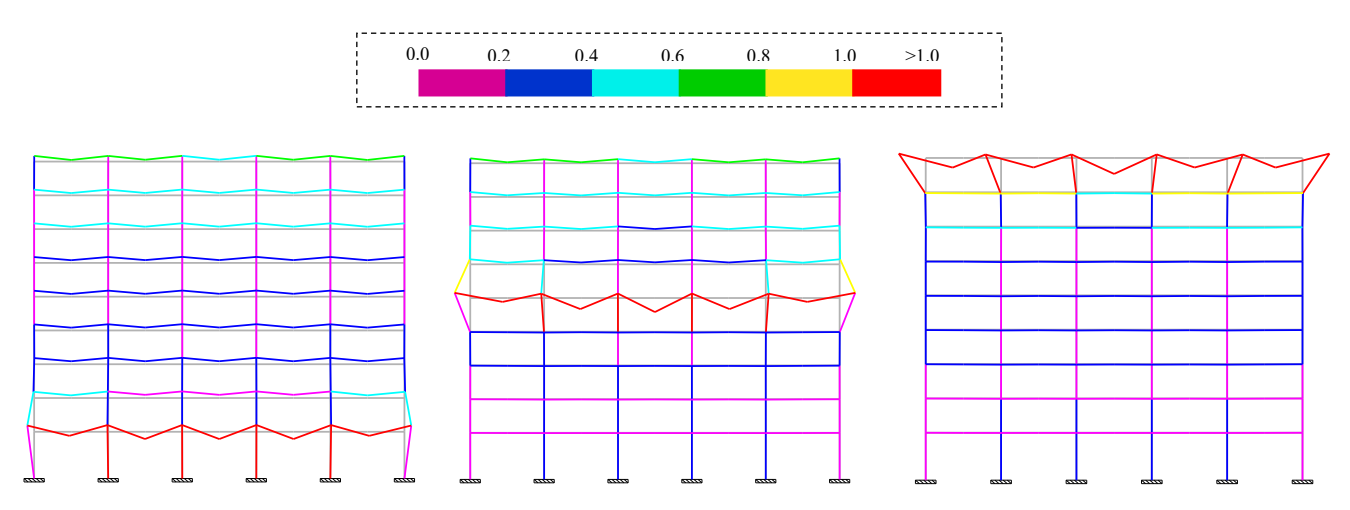


Fig. 20. Deformation and DCR of the elements in each scenario for nine-story steel frame.

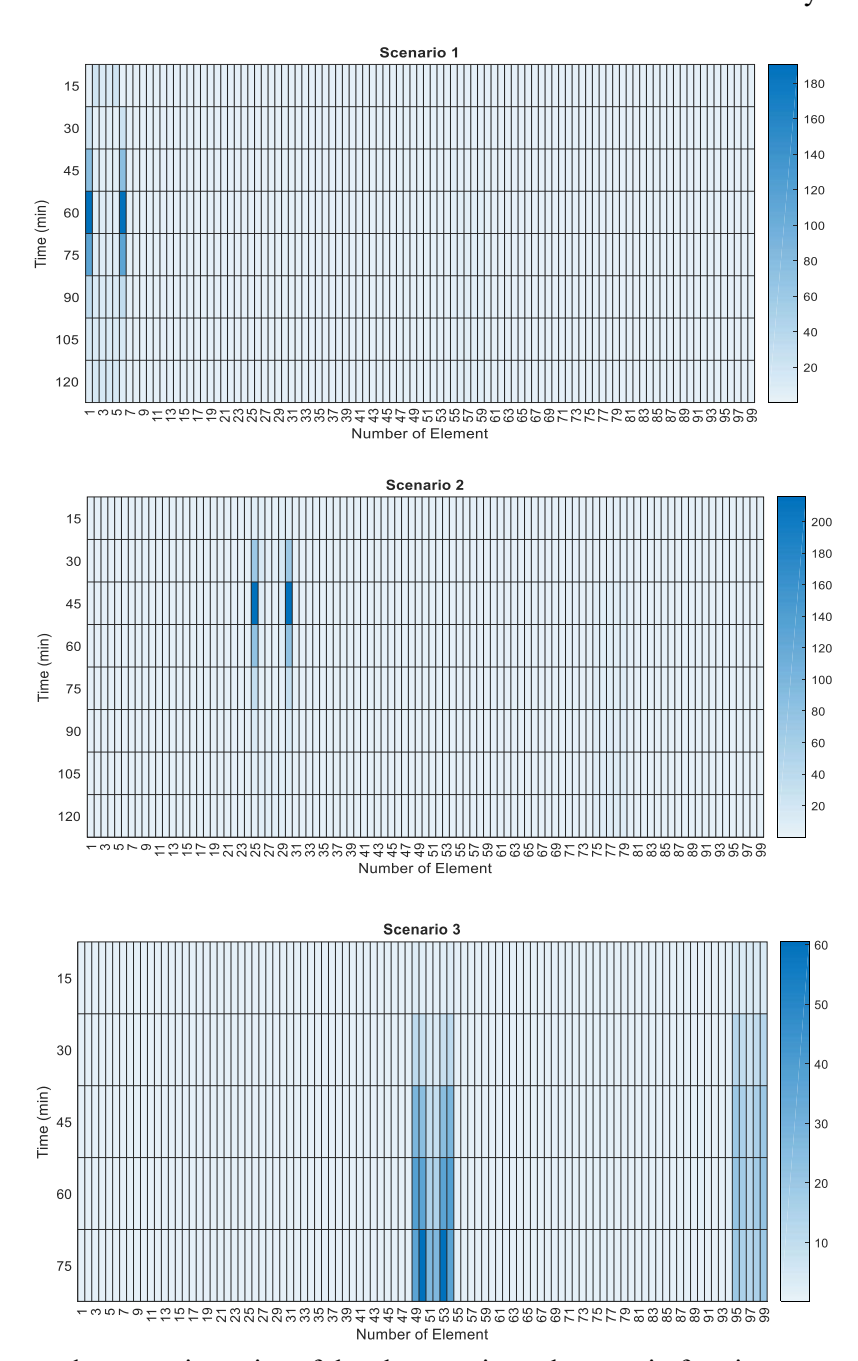


Fig. 21. Demand to capacity ratios of the elements in each scenario for nine-story steel frame.

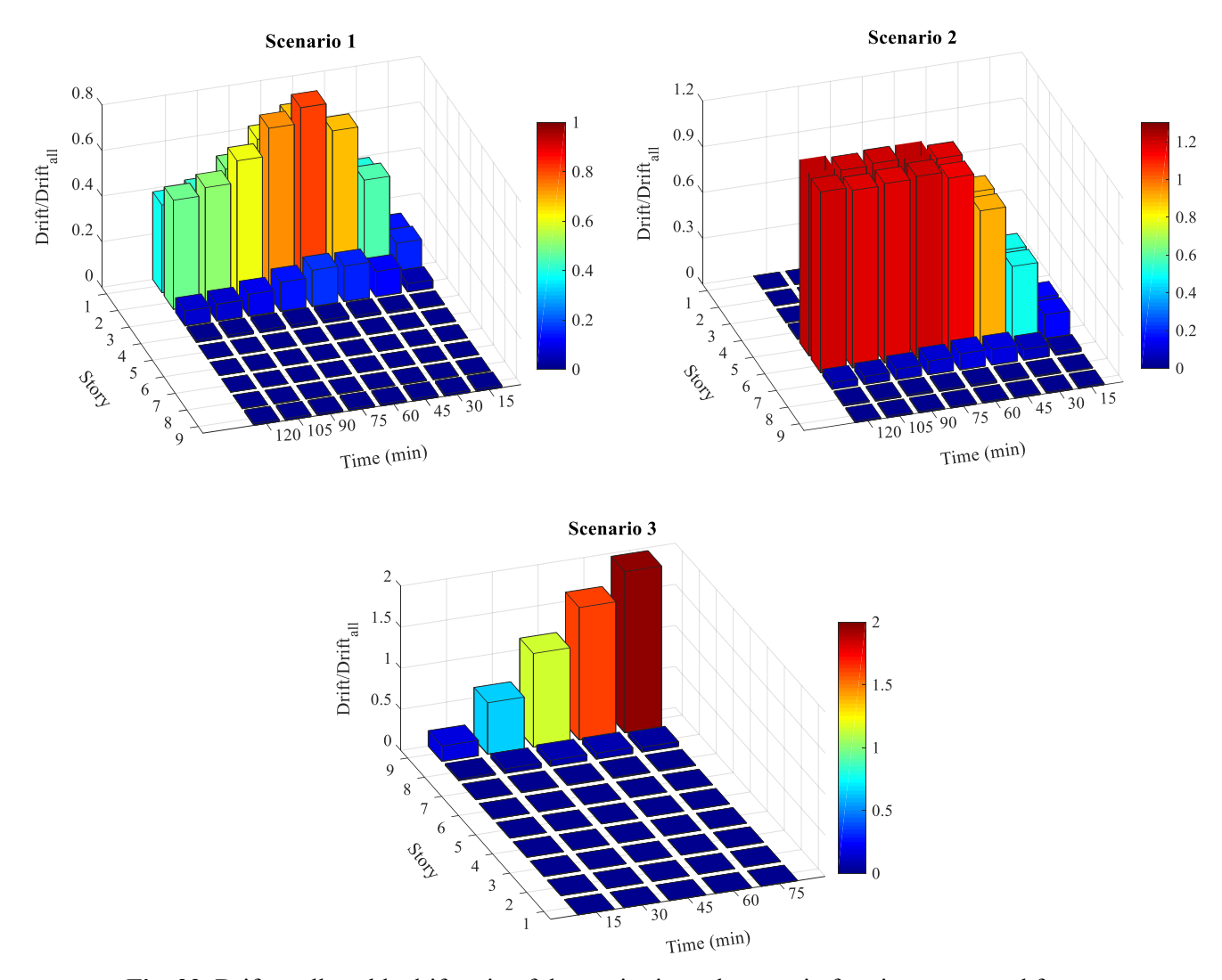


Fig. 22. Drift to allowable drift ratio of the stories in each scenario for nine-story steel frame.

The critical scenario for the nine-story frame was determind by evaluating the critical conditions in each story under fire. The evaluation of scenarios 1, 2, and 3 of the nine-story frame reveals that the most critical condition regarding beam deflection arises in scenario 2. By comparing the beam deflection results of considered scenarios can observe the fifth story is the most critical in terms of beam failure. Because the beams of this story failed in a shorter time and also experienced greater deflection that the sections of the beams also significantly can influence this problem.

Additionally, the demand-to-capacity ratio values of the structural members in scenario 2 exceed the established threshold of 1.0 more quickly than the other stories. In this scenario, the columns exhibit the highest DCR values over a shortened time frame, highlighting that the fifth story presents a greater risk compared to the other levels of the structure. Moreover, the ratio of drift to allowable drift show that in scenario 2, this ratio has exceeded its permissible limit over short time intervals. Excessive displacement in the mid-level stories of a nine-story frame can result in the development of a soft story, potentially compromising the structural integrity and leading to failure.

5. Conclusions

This study investigated the performance of three- and nine-story steel moment frames under various fire scenarios, with a focus on identifying critical conditions and understanding the structural behavior during

fire exposure. The fire duration in each scenario was considered to be 120 minutes at a temperature of 1050°C. Key parameters such as mid-span beam deflection, DCR (Demand-to-Capacity Ratio) of beams and columns, and story drift were analyzed to evaluate the structural response. The main findings of this study are summarized as follows:

- The study identified critical fire scenarios for each frame, which can significantly contribute to improving fire-resistant design methods for steel moment frames. For instance, scenarios 3, 6, and 9 were found to be critical for the first, second, and third stories of the three-story frame, respectively. The first story was found to be the most vulnerable, with beams failing in less than 90 minutes under fire exposure.
- The first story of the three-story frame and the fifth story of the nine-story frame were identified as the most vulnerable to fire-induced failure.
- Columns were found to be particularly critical, exhibiting the highest DCR values and failing faster than other structural members.
- Fire scenarios in lower or mid-level stories were observed to propagate significant displacements to other levels, increasing the overall risk of structural collapse.
- The drift to allowable-drift ratio emerged as a key indicator of structural vulnerability, with higher ratios signaling a greater risk of failure.
- Symmetry in both geometry and fire loading resulted in symmetrical behavior of structural members, suggesting that modeling and analyzing only half of the structure can be sufficient for design and evaluation purposes.
- In the three- and nine-story frame, the maximum mid-span deflection of beams reached 293.58 mm in scenario 4 and 551.22 mm in scenario 3, respectively.
- Columns exhibited the highest DCR values, exceeding the allowable limit of 1.0 in less than 90 minutes for the three-story frame and less than 80 minutes for the nine-story frame.
- Future studies could explore the effects of different fire temperatures and durations on the structural performance of steel frames, as these factors may vary in real-world fire incidents.
- The DCR drift in the three-story frame exceeded the permissible limit in scenarios 1, 2, and 3, with the highest drift observed in the first story, propagating significant displacement to upper levels. In the nine-story frame, the drift-to-allowable-drift ratio in scenario 2 exceeded the permissible limit, indicating a higher risk of soft-story formation in mid-level stories.
- Investigating the behavior of composite structures under fire conditions could provide additional insights into improving fire-resistant designs.

Funding

This research did not receive any specific grant from funding agencies in the public, commercial, or not-for-profit sectors.

Conflicts of interest

We wish to confirm that there are no known conflicts of interest associated with this publication. We confirm that the manuscript has been read and approved by all named authors and that there are no other persons who satisfied the criteria for authorship but are not listed. We further confirm that the order of authors listed in the manuscript has been approved by all of us.

Authors contribution statement

Arezoo Asaad Samani: Conceptualization; Data curation; Formal analysis; Investigation; Methodology; Software; Validation; Writing – original draft

Seyed Rohollah Hoseini Vaez: Conceptualization, Methodology, Supervision, Writing - Review & Editing.

References

- [1] Moradi M, Tavakoli HR, Abdollahzadeh G. Comparison of Steel and Reinforced Concrete Frames' Durability under Fire and Post-Earthquake Fire Scenario. Civil Engineering Infrastructures Journal 2021;54:145–68. https://doi.org/10.22059/CEIJ.2020.292639.1628.
- [2] Alasiri MR, Chicchi R, Varma AH. Post-earthquake fire behavior and performance-based fire design of steel moment frame buildings. Journal of Constructional Steel Research 2021;177:106442. https://doi.org/10.1016/J.JCSR.2020.106442.
- [3] Moradi M, Tavakoli HR, Abdollahzade GHR. Collapse Probability Assessment of a 4-Story RC Frame under Post-Earthquake Fire Scenario. Civil Engineering Infrastructures Journal 2022;55:121–37. https://doi.org/10.22059/CEIJ.2021.313241.1718.
- [4] Masoumi-Zahandeh F, Hoseinzadeh M, Rahimi S. Investigation of the Behavior of Buckling-Restrained Steel Plate Shear Wall under Fire Loading 2021;7:173-188 [In persian]. https://doi.org/10.22091/cer.2021.7372.1298.
- [5] Jiang J, Li GQ, Usmani A. Progressive Collapse Mechanisms of Steel Frames Exposed to Fire. Http://DxDoiOrg/101260/1369-4332173381 2016;17:381–98. https://doi.org/10.1260/1369-4332.17.3.381.
- [6] Jiang J, Li GQ, Usmani A. Progressive collapse mechanisms of steel frames exposed to fire. Advances in Structural Engineering 2014;17:381–98. https://doi.org/10.1260/1369-4332.17.3.381.
- [7] Shakeri J, Abdollahzadeh G. Seismic Rehabilitation of Tall Steel Moment Resisting Frames Damaged by Fire with SMA-Based Hybrid Friction Damper. International Journal of Steel Structures 2020;20:46–66. https://doi.org/10.1007/S13296-019-00270-Y/METRICS.
- [8] Pourkeramat P, Ghiasi V, Mohebi B. The Effect of Post-Earthquake Fire on the Performance of Steel Moment Frames Subjected to Different Ground Motion Intensities. International Journal of Steel Structures 2021 21:4 2021;21:1197–209. https://doi.org/10.1007/S13296-021-00496-9.
- [9] Heshmati M, Aghakouchak AA. Collapse analysis of regular and irregular tall steel moment frames under fire loading. The Structural Design of Tall and Special Buildings 2020;29:e1696. https://doi.org/10.1002/TAL.1696.
- [10] Alisawi AT, Collins PEF, Cashell KA. Nonlinear Analysis of a Steel Frame Structure Exposed to Post-Earthquake Fire. Fire 2021, Vol 4, Page 73 2021;4:73. https://doi.org/10.3390/FIRE4040073.
- [11] Chaboki M, Heshmati M, Aghakouchak AA. Investigating the behaviour of steel framed-tube and moment-resisting frame systems exposed to fire. Structures 2021;33:1802–18. https://doi.org/10.1016/J.ISTRUC.2021.05.053.
- [12] Ali AM, Akhaveissy AH, Abbas B. Fire Behavior of Lightweight Reinforced Concrete Deep Beams and Enhanced Structural Performance via Varied Stirrup Spacing An Integrated Study. Journal of Rehabilitation in Civil Engineering 2024;12:132–51. https://doi.org/10.22075/JRCE.2023.31484.1889.
- [13] Gernay T, Khorasani NE, Garlock M. Fire Fragility Functions for Steel Frame Buildings: Sensitivity Analysis and Reliability Framework. Fire Technology 2019;55:1175–210. https://doi.org/10.1007/s10694-018-0764-5.
- [14] Karimpour S, Madandous R, Ranjbar MM, Bengar A, Karimpour; S. An Experimental Study on Bond Behavior of Rebar and High-Performance Fiber Reinforced Cementitious Composite (HPFRCC) at High Temperatures. Journal of Rehabilitation in Civil Engineering 2024;12:77–91. https://doi.org/10.22075/JRCE.2023.29856.1810.

- [15] Moradi M, Tavakoli HR, Abdollahzadeh G. Probabilistic assessment of failure time in steel frame subjected to fire load under progressive collapses scenario. Engineering Failure Analysis 2019;102:136–47. https://doi.org/10.1016/J.ENGFAILANAL.2019.04.015.
- [16] Shahhoseini MR, Sharbatdar MK, Kheyroddin A. Experimental Investigation of Strength and Durability Properties of Concretes Cast with Heated Zeolite. Civil Infrastructure Researches 2024;10:35-50 [In persian].
- [17] Covi P, Tondini N, Sarreshtehdari A, Elhami-Khorasani N. Development of a novel fire following earthquake probabilistic framework applied to a steel braced frame. Structural Safety 2023;105:102377. https://doi.org/10.1016/J.STRUSAFE.2023.102377.
- [18] Jiang J, Usmani A. Modeling of steel frame structures in fire using OpenSees. Computers & Structures 2013;118:90–9. https://doi.org/10.1016/J.COMPSTRUC.2012.07.013.
- [19] Jiang J, Li G-Q, Usmani A. Influence of fire scenarios on progressive collapse mechanisms of steel framed structures. Steel Construction 2014;7:169–72. https://doi.org/10.1002/STCO.201410033.
- [20] Elhami Khorasani N, Garlock MEM, Quiel SE. Modeling steel structures in OpenSees: Enhancements for fire and multi-hazard probabilistic analyses. Computers & Structures 2015;157:218–31. https://doi.org/10.1016/J.COMPSTRUC.2015.05.025.
- [21] Jiang J, Li GQ, Usmani A. Effect of Bracing Systems on Fire-Induced Progressive Collapse of Steel Structures Using OpenSees. Fire Technology 2014 51:5 2014;51:1249–73. https://doi.org/10.1007/S10694-014-0451-0.
- [22] Ren W. Behaviour of Steel Frames Exposed to Different Fire Spread Scenarios. International Journal of Steel Structures 2020;20:636–54. https://doi.org/10.1007/S13296-020-00311-X/METRICS.
- [23] Jiang L, Jiang Y, Zhang Z, Usmani A. Thermal Analysis Infrastructure in OpenSees for Fire and its Smart Application Interface Towards Natural Fire Modelling. Fire Technology 2021;57:2955–80. https://doi.org/10.1007/S10694-020-01071-0/METRICS.
- [24] Qiu J, Jiang L, Anwar Orabi M, Usmani A, Li G. A computational approach for modelling composite slabs in fire within OpenSees framework. Engineering Structures 2022;255:113909. https://doi.org/10.1016/J.ENGSTRUCT.2022.113909.
- [25] Mortazavi SJ, Mansouri I, Awoyera PO, Hu JW. Comparison of thermal performance of steel moment and eccentrically braced frames. Journal of Building Engineering 2022;49:104052. https://doi.org/10.1016/J.JOBE.2022.104052.
- [26] Chen C, Jiang L, Qiu J, Orabi MA, Chan WS, Usmani A. OpenSees development for modelling timber structural members subjected to realistic fire impact. Fire and Materials 2023;47:461–78. https://doi.org/10.1002/FAM.3115.
- [27] Mortazavi SJ, Mansouri I, Farzampour A, Retzepis E, Hu JW. Evaluation of the Fire Behavior of Low-Rise Eccentrically Braced Frame Structures Under Different Fire Scenarios. Fire Technology 2024;60:3499–528. https://doi.org/10.1007/S10694-024-01587-9/FIGURES/16.
- [28] Opensees for fire by LimingXLiming n.d. https://openseesforfire.github.io/ (accessed February 7, 2025).
- [29] BS 476-20: Fire tests on building materials and structures. British Standard, Institution, B.S.; 1987.
- [30] ASTM E119: Standard Test Methods for Fire Tests of Building Construction and Materials. West Conshohocken, PA; 2016.
- [31] Buchanan AH and AKA. Structural design for fire safety. John Wiley & Sons; 2017.
- [32] ISO 834 Standard: Fire-resistance tests Elements of building construction Part 1: General requirements. 1999.
- [33] Structural Fire Engineering. American Society of Civil Engineers (ASCE); 2018.
- [34] EN 1993-1-2: Eurocode 3-Design of steel structures. 2005.
- [35] Karimi F, Hoseini Vaez SR. Two-stage optimal seismic design of steel moment frames using the LRFD-PBD method. Journal of Constructional Steel Research 2019;155:77–89. https://doi.org/10.1016/J.JCSR.2018.12.023.
- [36] ANSI/AISC 360-16 An American National Standard: Specification for Structural Steel Buildings. 2016.